

18.9 %-EFFICIENT SCREEN-PRINTED SOLAR CELLS APPLYING A PRINT-ON-PRINT PROCESS

Helge Hannebauer¹, Tom Falcon², Rene Hesse¹, Thorsten Dullweber¹, and Rolf Brendel^{1,3}

¹Institute for Solar Energy Research Hamelin (ISFH), Am Ohrberg 1, D-31860 Emmerthal, Germany

²DEK Printing Machines Ltd, 11 Albany Road, Weymouth, DT4 9TH, U.K.

³Department of Solar Energy, Institute of Solid-State Physics, Leibniz Universität Hannover, Appelstrasse 2, D-30167 Hannover, Germany

ABSTRACT: We investigate different process conditions of the print-on-print Ag front side metallization such as Ag pastes and screen aperture. The print-on-print process reduces the Ag finger width down to 70 μm . The application of the optimized print-on-print process to industrial type large area screen-printed solar cells displays conversion efficiencies up to 18.9 % compared to 18.5 % efficiency with standard single printed 107 μm wide Ag fingers. The efficiency improvement is caused by an improved short circuit current of up to 37.4 mA/cm^2 which is explained by the reduced shadowing loss. However, we find a strong dependence of the solar cell parameters on the print-on-print process conditions.

Keywords: Metallization, Screen Printing, Shading

1 INTRODUCTION

In today's industrial silicon solar cell production, screen-printing of the silver front contact and aluminium rear contact is the most commonly applied metallization [1]. One option to increase the conversion efficiency of screen-printed solar cells is to reduce the finger width of the silver front contacts in order to reduce the shadowing loss and hence increase the short circuit current (J_{sc}). However, in case of standard single printed Ag fingers a reduced finger width might lead to an increased finger line resistance as well as finger interruptions. The print-on-print (PoP) process consisting of two consecutive screen printing steps has the potential to achieve a reduced finger width in combination with a high aspect ratio compared to standard single printed silver fingers. Previous work on print-on-print demonstrated finger width down to 74 μm [2] and aspect ratios from 0.33 [3] up to 0.45 [2]. In the first PoP print step a silver paste is used to provide a good contact to the emitter. The second printing step is highly accurately aligned on the first print step and might use a different Ag paste which provides a low line resistance. Conversion efficiency improvements of up to 0.2 % for PoP cells compared to single printed cells [4, 5] have been reported.

In this paper, we investigate the impact of different silver pastes and screen apertures on the resulting finger width as well as the contact and line resistance of the silver fingers. We use two different screen apertures for the first and the second print instead of using the same aperture for both printing steps [2, 3, 5]. We apply the different PoP processes to solar cells and compare the resulting solar cell parameters to standard single printed solar cells.

2 EXPERIMENTAL SETUP

2.1 Cell Processing

We use $125 \times 125 \text{ mm}^2$ p -type 2 Ωcm Cz silicon wafers with an initial thickness of 210 μm . The schematic drawing of the final solar cell is shown in Fig. 1. On the textured surface a SiN_x antireflective coating passivates a homogeneously diffused phosphorous emitter of 50 Ω/\square sheet resistivity. The silver front contact and the aluminium rear contact are deposited by screen-printing

using a DEK PVP1200 production type screen printer. Afterwards, the wafers are fired in a conveyor belt furnace followed by a laser edge isolation. The PoP screen printing process consists of the following process steps:

- 1) screen printing of the bottom layer Ag paste Ag1, which provides a good contact resistance to the emitter
- 2) drying at 200 $^\circ\text{C}$
- 3) screen printing of the Ag paste Ag2 on top of paste Ag1 in order to reduce line resistance
- 4) drying at 200 $^\circ\text{C}$.

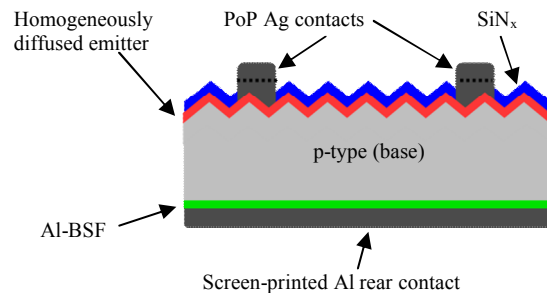


Figure 1: Schematic drawing of the industrial type silicon solar cell with print-on-print Ag front contacts.

We use a two bus bar 60 finger layout for PoP and a two busbar 50 finger design for single print. We increase the finger number for PoP in order to reduce resistive losses due to the smaller finger width and to obtain similar series resistances for PoP cells compared to single printed cells.

2.2 PoP process variations

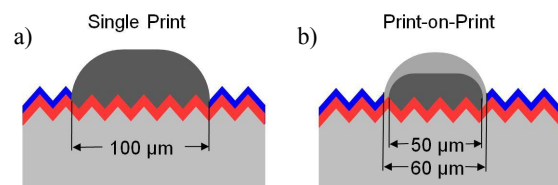


Figure 2: Schematic drawing of a) single print reference process b) PoP process with 50 μm aperture for print 1 and 60 μm for print 2.

For the PoP process we use two different screens with finger apertures of 50 μm and 60 μm to investigate the impact of wider and narrower second print. We investigate pastes B1 and B2 as well as pastes C1 and C2. The index 1 refers to the bottom silver paste, the index 2 to the top silver paste of the PoP process. Paste A for the single print is used as a reference. A comparison between single print and PoP is shown as a schematic drawing in Fig. 2.

Table I: Summary of the different experimental groups investigated in this paper.

Split group	Screen aperture and silver paste
PoP1	Bottom: 50 μm , Paste C1 Top: 60 μm , Paste C2
PoP2	Bottom: 60 μm , Paste C1 Top: 50 μm , Paste C2
PoP3	Bottom: 50 μm , Paste B1 Top: 60 μm , Paste B2
SP	100 μm , Paste A

Table I shows the different experimental groups. In PoP1 we print silver paste C1 first with a screen aperture of 50 μm and paste C2 as top layer with a screen aperture of 60 μm . In PoP2 we use silver paste C1 with a screen aperture of 60 μm for the first print and paste C2 with a screen aperture of 50 μm for the second print. PoP3 uses paste B1 as bottom layer with 50 μm screen aperture and paste B2 for the top layer using a screen aperture of 60 μm . As a reference process with single print (SP), group SP is printed with a screen aperture of 100 μm using paste A.

3 EXPERIMENTAL RESULTS

3.1 Ag finger properties

In table II we summarize the Ag finger properties. The finger width and the aspect ratio (AR) are measured with a light optical microscope after firing. The single print (group SP) shows an AR of 0.22 with finger width of 114 μm . In contrast, the groups PoP1 to PoP3 demonstrate strongly reduced finger width between 68 μm and 78 μm with an AR between 0.39 and 0.44.

Table II: Aspect ratio (AR) and average finger width for three different print-on-print processes compared to a standard single print front side Ag metallization.

Process group	Measured finger width	AR
PoP1	68.0 μm	0.44
PoP2	78.1 μm	0.39
PoP3	70.8 μm	0.42
SP	114.5 μm	0.22

Fig. 3 shows scanning electron microscope (SEM) images of the groups PoP1 and SP. Comparing the best print-on-print process in fig. 3a) with our single print reference process in fig 3b), we see a reduction of the finger width from 107 μm to 55 μm using PoP.

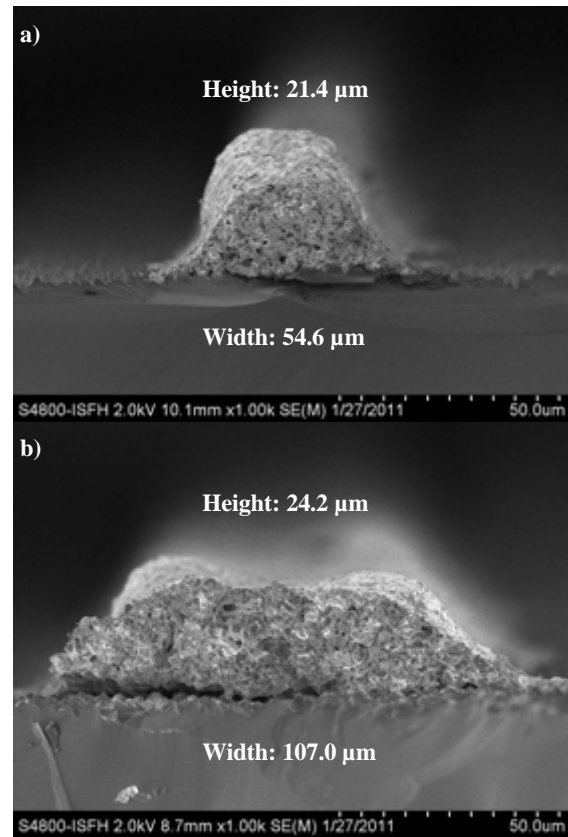


Figure 3: SEM images of (a) the PoP Ag finger with process conditions of PoP1 in table I and a finger width of 55 μm (b) standard single printed Ag finger with a width of 107 μm (group SP in table I).

3.2 Solar Cell Results

Table III: Solar cell parameters of three different print-on-print processes compared to the single print reference process.

Process group	η [%]	J_{sc} [mA/cm^2]	V_{oc} [mV]	FF [%]	R_s [Ocm^2]
PoP1	18.9	37.4	634	79.7	0.6
PoP2	18.3	36.9	624	79.5	0.6
PoP3	18.1	36.8	622	79.1	0.7
SP	18.5	37.0	633	79.2	0.6

Applying the process flow of section 2.1, we fabricate solar cells with the different Ag front side printing parameters described in table I. Table III shows the IV measurement results of the best solar cells of the three different PoP processes and the single print process. The PoP process improves the conversion efficiency up to 18.9 % applying the process conditions of group PoP1, which represents an improvement of 0.4 % compared to the standard single print solar cell with 18.5 % conversion efficiency. The improved efficiencies of group PoP1 have been repeated several times with different process batches resulting in an average conversion efficiency of 18.7 % with a standard deviation of ± 0.12 %. The efficiency improvement is mainly due to an increased short circuit current of up to 37.4 mA/cm^2 . Based on screen layout parameters, we estimate that the reduced finger width with PoP reduces

the shadowing loss from 6.7 % for SP down to 5.4 %, which explains the J_{sc} improvement for group PoP1. However, the print-on-print groups PoP2 and PoP3 in table III show conversion efficiencies of only 18.1 % and 18.3 % due to lower V_{oc} , J_{sc} , and FF compared to group PoP1. The root cause for these solar cell parameter dependencies on the printing conditions is analysed in the following subsections.

3.3 Investigation of the Ag finger conductivity and contact resistance

In order to analyse the root cause of the FF variations in table III, we investigate the specific contact resistance and line resistance of the different printing conditions. Table IV shows the FF and series resistance of the solar cells of table III. The specific contact resistance (ρ_c) was measured by the transfer length method (TLM) [6, 7] on solar cells. The specific line resistance (ρ_l) has been deduced by measuring the cross section area of the finger with an optical profilometer as well as the line resistance measured on a 2.2 cm wide TLM sample for each group. The print-on-print process using the paste combination C1 and C2 (group PoP1 & PoP2) slightly improves ρ_l in comparison to the single print process. This improvement is due to the fact that we use two different silver pastes for PoP and the second layer should provide a lower bulk resistance than other single print pastes. In contrast, group PoP3 shows the highest values for ρ_l and ρ_c .

Table IV: Electrical parameters of the three different PoP groups and the single print group.

Process group	FF [%]	R_s [Ωcm^2]	Specific contact resistance ρ_c [$\text{m}\Omega\text{cm}^2$]	Specific line resistance ρ_l [$\mu\Omega\text{cm}$]
PoP1	79.7	0.6	2.33	2.45
PoP2	79.5	0.6	3.51	2.48
PoP3	79.1	0.7	9.95	2.69
SP	79.2	0.6	1.45	2.55

Following the formulas of [8], we calculate the total series resistance of the solar cells of PoP1 and SP based on the results of table IV and find a good agreement to the measured R_s values of table IV. In general, the PoP cells have higher contact resistance R_c and line resistance R_l compared to SP cells. This is compensated by the increased finger number which reduces the series resistance of the emitter R_e .

3.4 Correlation of J_{sc} to finger width

In order to analyse the J_{sc} dependence shown in table III on the different printing processes of table I, we calculated the dependence of the J_{sc} on the finger width. We are taking into account the shadowing loss of the fingers as well as the bus bars by applying equation (1).

$$J_{sc} = J_{sc,0} \cdot \left(1 - \frac{w_f \cdot l_f \cdot n_f + A_{BB}}{A_{cell}} \right) \quad (1)$$

Here, w_f is the measured finger width, l_f the finger length, n_f the number of fingers on the cell, A_{BB} the bus bar area of the screen design, and A_{cell} the area of the solar cell. $J_{sc,0}$ corresponds to the expected short circuit current with no metallization on the front side and is used as a fit parameter in equation (1) in order to represent the

J_{sc} values of the single printed cells (group SP in table I) for different finger width.

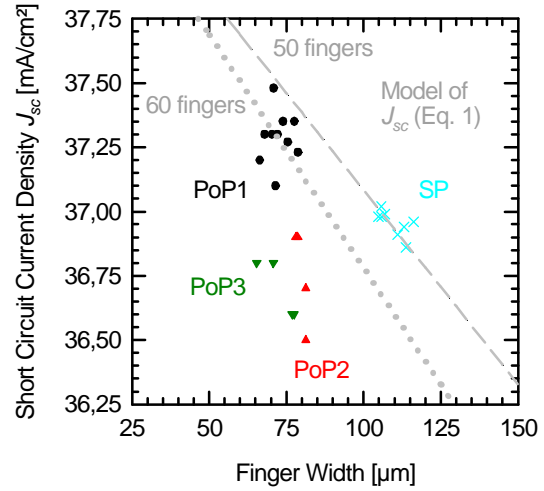


Figure 4: Short circuit current density J_{sc} versus the measured finger width of several cells of the four groups of table I. The lines are calculated applying equation 1 for a 50 finger (SP) and a 60 finger (PoP) layout.

Figure 4 shows the measured J_{sc} versus the measured finger width of several solar cells of groups PoP1 – PoP3 and SP. Equation (1) is plotted for both the 50 finger screen design ($n_f = 50$), which represents the single print results, and the 60 finger screen design ($n_f = 60$), which refers to the print-on-print cells. The best fit of equation (1) with respect to the single printed cells is obtained with $J_{sc,0} = 39.65 \text{ mA/cm}^2 \pm 0.1 \text{ mA/cm}^2$. The measured J_{sc} values of the print-on-print cells of group PoP1 are well fitted by equation (1). In contrast, the measured J_{sc} values of the PoP groups 2 and 3 are considerably smaller compared to the calculated J_{sc} values applying equation (1).

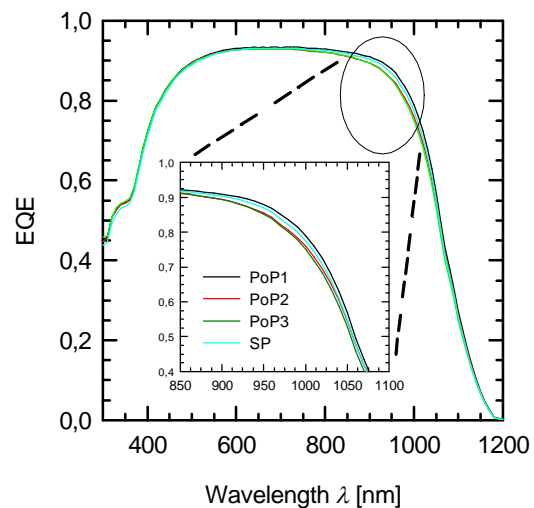


Figure 5: External quantum efficiency (EQE) of the solar cells in table III.

In order to investigate the strong dependence of the short circuit current density and the open circuit voltage on the printing conditions, we analyse the external quantum efficiency (EQE) of the solar cells shown in table III. The

EQE curves in Fig. 5 of the different process groups differ in the long wavelength regime $\lambda > 800$ nm. The solar cells with the highest J_{sc} also show the highest EQE at $\lambda = 900$ nm which would indicate *e.g.* a difference in the rear surface recombination velocity. However, it is not yet clear if the difference in the rear surface recombination velocity is really caused by the different Ag printing conditions and hence requires further investigation.

4 CONCLUSIONS

We have evaluated the print-on-print process for industrial type screen-printed silicon solar cells. The PoP process reduces the finger width down to 70 μm , which increases the J_{sc} and hence the efficiency from 18.5 % for single print up to 18.9 % for PoP. The J_{sc} improvement is in accordance with a model of the shadowing loss. However, the PoP process parameters such as screen aperture and type of Ag paste show a strong impact on the solar cell parameters even though the finger width is very similar. The root cause analysis requires further investigations.

5 REFERENCES

- [1] E. Kossen et al, Proceedings 25th European Photovoltaic Solar Energy Conference, (2010) 2099
- [2] M. Galiazzo et al, Proceedings 25th European Photovoltaic Solar Energy Conference, (2010) 2338
- [3] H. Kerp et al, Proceedings 25th European Photovoltaic Solar Energy Conference, (2010) 2460
- [4] T. Falcon, Proceedings 25th European Photovoltaic Solar Energy Conference, (2010) 1651
- [5] T. Pham et al, Proceedings 25th European Photovoltaic Solar Energy Conference, (2010) 2378
- [6] D. Meier et al, IEEE Transactions on Electron Devices, Vol. ED-31, No.5, (1984) 647
- [7] S. Cohen, Thin Solid Films, Vol.104, (1983) 361
- [8] A. Mette, Phd thesis, University of Freiburg, (2007)